Quantum Spin Stabilized Magnetic Levitation

C. C. Rusconi,[1,2] V. Pöchhacker,[1,2] K. Kustura,[1,2] J. I. Cirac,[3] and O. Romero-Isart[1,2]

[1]*Institute for Quantum Optics and Quantum Information of the Austrian Academy of Sciences, A-6020 Innsbruck, Austria*
[2]*Institute for Theoretical Physics, University of Innsbruck, A-6020 Innsbruck, Austria*
[3]*Max-Planck-Institut für Quantenoptik, Hans-Kopfermann-Straße 1, D-85748 Garching, Germany*

We theoretically show that, despite Earnshaw's theorem, a nonrotating single magnetic domain nanoparticle can be stably levitated in an external static magnetic field. The stabilization relies on the quantum spin origin of magnetization, namely, the gyromagnetic effect. We predict the existence of two stable phases related to the Einstein–de Haas effect and the Larmor precession. At a stable point, we derive a quadratic Hamiltonian that describes the quantum fluctuations of the degrees of freedom of the system. We show that, in the absence of thermal fluctuations, the quantum state of the nanomagnet at the equilibrium point contains entanglement and squeezing.

According to the Einstein–de Haas and Barnett effects [1,2], a change in the magnetization of an object is accompanied by a change in its rotational motion. Specifically, if the magnetic moment of a magnet is varied by a single Bohr magneton, it must rotate with an angular frequency $\hbar/I$ about the magnetic moment axis to conserve angular momentum. Here, I is its moment of inertia about the rotation axis. For a Cobalt sphere of radius R, this corresponds to a frequency $\hbar/I \approx 2\pi \times 10^6$ Hz$/(R[\text{nm}])^5$, where $R[\text{nm}]$ is the radius in nanometers. This clear manifestation of the quantum spin origin of magnetization, as prescribed by the gyromagnetic relation, is hence boosted at the nanoscale [3–5].

In this Letter, we explore the role of the quantum spin origin of magnetization in magnetic levitation. Earnshaw's theorem [6], very relevant in this context, prevents magnetic levitation of a nonrotating ferromagnet in a static magnetic field. The theorem can be circumvented by mechanically spinning the magnet, as is neatly demonstrated by the Levitron [7–10], which is a magnetic top of a few centimeters. At the single atom level, magnetic trapping with static fields is also possible by exploiting the fast Larmor precession of its quantum spin [11,12]. In this case, the atom is, from the mechanics point of view, a point particle without rotational degrees of freedom. A magnetic nanoparticle lies between the Levitron and the atom, as both its rotational degrees of freedom and the quantum spin origin of magnetization have to be accounted for. Can a nonrotating magnetic nanoparticle, despite Earnshaw's theorem, be stably levitated with static magnetic fields?

We show in this Letter that this is the case. Specifically, we predict two stabilization mechanisms that crucially rely on the quantum spin origin of the magnetic moment. At low (large) magnetic fields, the Einstein–de Haas effect (the Larmor precession of its magnetic moment) stabilizes levitation. These results are obtained by deriving a quadratic

Hamiltonian which describes the linearized dynamics of the degrees of freedom of the magnet (center-of-mass motion, rotation, and magnetization dynamics) around the equilibrium point. We further show that, in the absence of thermal fluctuations, the equilibrium state exhibits both quantum entanglement and squeezing of its degrees of freedom. As discussed in the conclusion, these results could be used to bring and control the rich physics of levitated nanomagnets in the quantum regime.

We consider a single magnetic domain nanoparticle (called a nanomagnet hereafter) in an external static magnetic field $\mathbf{B}(\mathbf{r})$. The nanomagnet is modeled [13] as a spherical rigid body of mass M and radius R, and with uniaxial magnetocrystalline anisotropy [14]. The dynamics are described in the body frame $O\mathbf{e}_1\mathbf{e}_2\mathbf{e}_3$, with $\mathbf{e}_3$ aligned to the direction of the anisotropy axis. The body frame is obtained from the laboratory frame $O\mathbf{e}_x\mathbf{e}_y\mathbf{e}_z$ by the rotation $R(\Omega)$, as defined in Ref. [15], where $\Omega = \{\alpha, \beta, \gamma\}$ represents the Euler angles. The Hamiltonian of the system in the body frame is given by [15]

$$\hat{H} = \frac{\hat{\mathbf{p}}^2}{2M} + \frac{\hbar^2}{2I}(\hat{\mathbf{J}} + \hat{\mathbf{S}})^2 - \hbar^2 D\hat{S}_3^2 + \hbar\gamma_0\hat{\mathbf{S}} \cdot \mathbf{B}(\hat{\mathbf{r}}, \hat{\Omega}). \quad (1)$$

Here, $\hat{\mathbf{J}} \equiv \hat{\mathbf{L}} + \hat{\boldsymbol{\mu}}/(\hbar\gamma_0)$ is the total angular momentum (excluding the center-of-mass angular momentum), $\hat{\mathbf{S}} \equiv -\hat{\boldsymbol{\mu}}/(\hbar\gamma_0)$ the spin angular momentum [16], $\hat{\mathbf{L}}$ the rigid body angular momentum, $\hat{\boldsymbol{\mu}}$ the magnetic moment operator, and $\gamma_0 > 0$ the gyromagnetic ratio [17]. The macrospin approximation is assumed, namely, that the total magnetization is constant, which results in $\hat{\mathbf{S}}^2 = S(S+1)\mathbb{1}$, with $S \equiv Nf$ for N identical spin f constituents of the nanomagnet [18]. The first (second) term in Eq. (1) represents the center-of-mass (rotational) kinetic energy of the nanomagnet. The third term represents the uniaxial magnetocrystalline anisotropy, whose strength is parametrized by

$D \equiv 4\pi R^3 k_a/(3\hbar^2 S^2)$, with k_a being the material-dependent anisotropy constant [18]. The last term represents the magnetic dipolar interaction, where $\mathbf{B}(\mathbf{r}, \Omega) \equiv R(\Omega)\mathbf{B}(\mathbf{r})$. Hereafter, we consider an Ioffe-Pritchard magnetic field, i.e., $\mathbf{B}(\mathbf{r}) = \mathbf{e}_x(B'x - B''xz/2) - \mathbf{e}_y(B'y + B''yz/2) + \mathbf{e}_z[B_0 + B''z^2/2 - B''(x^2 + y^2)/4]$, where B_0, B', and B'' are, respectively, the field bias, the gradient, and the curvature [19]. Gravity, which is assumed to be along the z axis, can be safely neglected since, throughout the Letter, the condition $Mg/(\mu B'') \ll (B_0/B'')^{1/2}, (B'/B'')$ is fulfilled, where g is the gravitational acceleration; see Ref. [20] for further details. The rotational angular momentum of the nanomagnet about the anisotropy axis is a constant of motion, $[\hat{L}_3, \hat{H}] = 0$ [15]. The degrees of freedom of the system—namely, the center-of-mass motion, the rotational motion, and the magnetization dynamics—are thus described by 12 independent dynamical variables (see Ref. [20] for further details). In the following, we address whether the nanomagnet can stably levitate for a given set of physical parameters of our model: mass density ρ_M, magnetization ρ_μ, k_a, R, B_0, B', and B''.

Let us first obtain the equilibrium configuration of the system. By writing the Heisenberg equations of motion for the nanomagnet in semiclassical approximation [20], the following relative equilibrium is found (see Fig. 1). (i) The center of mass is fixed at the center of the trap. (ii) The orientation is given by the body frame aligned to the laboratory frame ($\mathbf{e}_3 \| \mathbf{e}_z$) and rotating about $\mathbf{e}_3$ at the frequency $\omega_S \equiv -\hbar\langle\hat{L}_3\rangle/I$. (iii) The magnetic moment lies along the anisotropy axis $\mathbf{e}_3$ and is antialigned to the magnetic field $\mathbf{B}(0) = B_0\mathbf{e}_z$. The stability of this relative equilibrium is analyzed in the frame corotating with the system [20,21]. This is obtained via the unitary transformation $\hat{U} = \exp(-i\omega_S\hat{L}_3 t)$, which transforms $\hat{H}$ into $\hat{H} + \hbar\omega_S\hat{L}_3$.

The linear stability of the system is determined by the dynamics of the fluctuations of the degrees of freedom
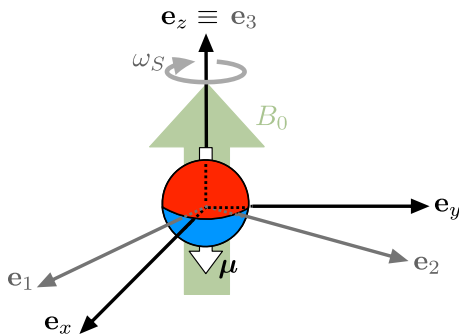

FIG. 1.   Relative equilibrium for a magnetically levitated nanomagnet. The nanomagnet is at the center of the trap and rotates about its magnetization axis at the constant frequency $\omega_S \equiv -\hbar\langle\hat{L}_3\rangle/I$. The magnetic moment lies along the anisotropy axis and is antialigned to $\mathbf{B}(0) = B_0\mathbf{e}_z$.

around the equilibrium. The evolution of small fluctuations can be described as a collection of interacting harmonic oscillators through the bosonization procedure presented in Ref. [15]. In the following, we provide the mapping between the observables and the bosonic operators and refer to Ref. [15] for its derivation and for further details. The fluctuations of the center-of-mass motion are described by three independent harmonic oscillators:

$$\hat{z} \equiv z_0(\hat{b}_z + \hat{b}_z^\dagger), \qquad \hat{p}_z \equiv \frac{i\hbar}{2z_0}(\hat{b}_z^\dagger - \hat{b}_z) \qquad (2)$$

for the motion along $\mathbf{e}_z$, and

$$\hat{r}_+ \equiv \sqrt{2}r_0(\hat{b}_R^\dagger + \hat{b}_L), \qquad \hat{p}_+ \equiv i\frac{\hbar}{\sqrt{2}r_0}(\hat{b}_L^\dagger - \hat{b}_R) \qquad (3)$$

for the transverse motion, where $\hat{r}_\pm = \hat{x} \pm i\hat{y}$ and $\hat{p}_\pm = \hat{p}_x \pm i\hat{p}_y$. Here, $z_0 \equiv \sqrt{\hbar/(2M\omega_Z)}$ and $r_0 \equiv \sqrt{\hbar/(2M\omega_T)}$ are the zero-point motions and $\omega_Z \equiv \sqrt{\hbar\gamma_0 B''S/M}$ and $\omega_T \equiv \sqrt{\hbar\gamma_0 S(B'^2 - B_0 B''/2)/MB_0}$ the trap frequencies. We introduced three bosonic modes with $[\hat{b}_i, \hat{b}_j^\dagger] = \delta_{ij}$ for $i, j = z, R, L$. The harmonic oscillators describing the fluctuations of the rotational degrees of freedom are obtained as follows. A Holstein-Primakoff mapping generalized to the case where $\hat{\mathbf{J}}^2$ is not conserved [22] leads to

$$\hat{J}_\uparrow = \hat{J}_\downarrow^\dagger \equiv \hat{J}_1 - i\hat{J}_2 = \sqrt{2J}\hat{k}^\dagger, \qquad (4)$$

$$\hat{J}_3 = -J - \sqrt{2J}(\hat{j} + \hat{j}^\dagger)/2 - \hat{j}^\dagger\hat{j}/2 + \hat{k}^\dagger\hat{k}. \qquad (5)$$

The k-bosonic mode ($[\hat{k}, \hat{k}^\dagger] = 1$) describes the fluctuations of $\hat{J}_3$ around $\langle\hat{J}_3\rangle = -J \equiv -I\omega_S/\hbar - S$. As discussed below, we assume $J \gg 1$. The j-bosonic mode ($[\hat{j}, \hat{j}^\dagger] = 1$) describes the fluctuations of $\hat{\mathbf{J}}^2$ around $\langle\hat{\mathbf{J}}^2\rangle = J(J + 1)$. Since the components of $\hat{\mathbf{J}}$ in the laboratory frame commute with $\hat{J}_3$ and $\hat{J}_{\downarrow\uparrow}$ [23], they need to be bosonized separately as

$$\hat{J}_+ = \hat{J}_-^\dagger \equiv \hat{J}_x + i\hat{J}_y = \sqrt{2J}\hat{m}^\dagger, \qquad (6)$$

$$\hat{J}_z = -J - \sqrt{2J}(\hat{j} + \hat{j}^\dagger)/2 - \hat{j}^\dagger\hat{j}/2 + \hat{m}^\dagger\hat{m}. \qquad (7)$$

The additional m-bosonic mode ($[\hat{m}, \hat{m}^\dagger] = 1$) represents the fluctuations of $\hat{J}_z$ around $\langle\hat{J}_z\rangle = -J$. The bosonization of the Euler angle operators is more involved [15]. Since $\hat{\Omega}$ appears in Eq. (1) only inside trigonometric functions, the Euler angle operators can be written as functions of the nine Wigner D-matrix tensor operators $\hat{\mathcal{D}}_{mk}^1$ with $m, k = \pm 1, 0$. The exact bosonization of these operators is given in Ref. [15] in terms of the $j - k - m$-bosonic modes. The fluctuations of the magnetic moment under the macrospin

approximation $[\hat{\mathbf{S}}^2 = S(S+1)\mathbb{1}$, with $S \gg 1]$ can be described by the standard Holstein-Primakoff approximation, namely [16,24],

$$\hat{S}_{\uparrow} = \hat{S}_{\downarrow}^{\dagger} \equiv \hat{S}_1 - i\hat{S}_2 = \sqrt{2S}\hat{s}, \quad (8)$$

$$\hat{S}_3 = S - \hat{s}^{\dagger}\hat{s}. \quad (9)$$

The s-bosonic mode describes fluctuations of $\hat{S}_3$ around $\langle \hat{S}_3 \rangle = S$. In summary, the fluctuations of the degrees of freedom of the nanomagnet around the equilibrium illustrated in Fig. 1 are described by seven bosonic modes.

Let us now derive the Hamiltonian describing the dynamics of these bosonic modes. Note that since $\hat{L}_3 = \hat{J}_3 + \hat{S}_3$ is a constant of motion, the bosonic modes are constrained by $\sqrt{2J}(\hat{j}^{\dagger} + \hat{j}) = \hat{j}^{\dagger}\hat{j}/2 - \hat{k}^{\dagger}\hat{k} - \hat{s}^{\dagger}\hat{s}$. Together with the assumption of a slowly rotating nanomagnet, namely, $|I\omega_S/\hbar| \ll S$, which implies $J \gg 1$, the bosonization procedure transforms $\hat{H} + \hbar\omega_S\hat{L}_3$ into a quadratic Hamiltonian that depends on six bosonic modes: $\hat{b}_z, \hat{b}_R, \hat{b}_L, \hat{m}, \hat{k}$, and $\hat{s}$. Terms containing the j mode, as well as nonquadratic terms, are of the order $(1/J)^{n/2}$ for $n = 1, 2, \ldots$, and they can thus be safely neglected. The quadratic Hamiltonian reads

$$\hat{H}_q \equiv \hat{H}_Z + \hat{H}_T = \frac{\hbar}{2}(\hat{\Psi}_Z^{\dagger}M_Z\hat{\Psi}_Z + \hat{\boldsymbol{\psi}}^{\dagger}C\hat{\boldsymbol{\psi}} + \hat{\boldsymbol{\psi}}C^*\hat{\boldsymbol{\psi}}^{\dagger}).$$
$$(10)$$

The first term describes the fluctuations of the center-of-mass motion along $\mathbf{e}_z$, where $\hat{\Psi}_Z = (\hat{b}_z, \hat{b}_z^{\dagger})^T$ and $M_Z = \omega_Z\mathbb{1}_2$. The second term describes the fluctuations of the other degrees of freedom, where $\hat{\boldsymbol{\psi}} \equiv (\hat{b}_R^{\dagger}, \hat{k}^{\dagger}, \hat{b}_L, \hat{m}, \hat{s})^T$ and

$$C \equiv \begin{pmatrix} \omega_- & g\eta & -\omega_+ & -g\eta & g \\ g\eta & \omega_k & g\eta & \omega_L\eta^2 & \omega_k\eta^{-1} \\ -\omega_+ & g\eta & \omega_- & -g\eta & g \\ -g\eta & \omega_L\eta^2 & -g\eta & -\omega_L\eta^2 & \omega_L\eta \\ g & \omega_k\eta^{-1} & g & \omega_L\eta & \omega_\mu \end{pmatrix}. \quad (11)$$

Here, we defined $\eta \equiv \sqrt{S/J}$, the Larmor frequency $\omega_L \equiv \gamma_0 B_0$, the anisotropy frequency $\omega_D \equiv \hbar DS$, the Einstein–de Haas frequency $\omega_I \equiv \hbar S/I$, the frequencies $\omega_k \equiv \omega_I + \omega_S - \omega_L\eta^2$, $\omega_\mu \equiv \omega_I + 2\omega_D - \omega_L$, and $\omega_\pm \equiv (\omega_T \pm \omega_Z^2/\omega_T)/2$, and the coupling strength $g \equiv \omega_L B' \sigma_T/B_0$. As shown below, the hierarchy between ω_L, ω_D, and ω_I plays a crucial role in the stability of the nanomagnet.

The linear stability of the equilibrium can be determined by the Heisenberg equations of motion

$$\partial_t\hat{\Psi}_Z = \frac{1}{i\hbar}[\hat{\Psi}_Z, \hat{H}_Z] \equiv iK_Z\hat{\Psi}_Z = i\sigma_z M_Z\hat{\Psi}_Z, \quad (12)$$

$$\partial_t\hat{\Psi} = \frac{1}{i\hbar}[\hat{\Psi}, \hat{H}_T] \equiv iK_T\hat{\Psi} = iGM_T\hat{\Psi}. \quad (13)$$

Here, $\sigma_z = \text{diag}(1, -1)$, $G \equiv \mathbb{1}_5 \otimes \sigma_z$, and $M_T = M_T^{\dagger}$ is given by rewriting $\hat{H}_T$ as $\hat{H}_T = \hbar\hat{\Psi}^{\dagger}M_T\hat{\Psi}/2$, where $\hat{\Psi} \equiv (\hat{b}_R, \hat{b}_R^{\dagger}, \hat{b}_L, \hat{b}_L^{\dagger}, \hat{m}, \hat{m}^{\dagger}, \hat{k}, \hat{k}^{\dagger}, \hat{s}, \hat{s}^{\dagger})^T$. The dynamics of the system are completely characterized by the characteristic polynomials of iK_Z and iK_T. Linear stability occurs when the roots of the polynomials have a zero real part [21]. The characteristic polynomial of iK_Z reads $P_Z(\lambda) = \lambda^2 + \omega_Z^2$, which has purely imaginary roots for $B'' > 0$. The matrix iK_T can be block diagonalized in two 5×5 complex conjugate blocks whose characteristic polynomial is given by $P_T(\lambda) = a_0 + a_1\lambda + a_2\lambda^2 + a_3\lambda^3 + a_4\lambda^4 + a_5\lambda^5$, where

$$a_0 \equiv -2\omega_D\omega_I\omega_L\omega_T^2,$$

$$a_1 \equiv i[\omega_D\omega_Z^2(\omega_S + \omega_I) + \omega_S\omega_L\omega_T^2],$$

$$a_2 \equiv -2\omega_D\omega_I\omega_L - \frac{1}{2}(2\omega_D - \omega_S)\omega_Z^2 - \omega_L\omega_T^2,$$

$$a_3 \equiv i\left[-2\omega_D(\omega_S + \omega_I) + \omega_S\omega_L + \frac{1}{2}\omega_Z^2\right],$$

$$a_4 \equiv 2\omega_D - \omega_S - \omega_L,$$

$$a_5 \equiv -i. \quad (14)$$

The analysis of $P_Z(\lambda)$ and $P_T(\lambda)$ as functions of the physical parameters of the problem provides the stability diagram of a magnetically levitated nanomagnet, as discussed below. These polynomials can be alternatively obtained either by using classical equations of motion or via the linearized Heisenberg equations of motion in semiclassical approximation without performing the bosonization; see Ref. [20]. Such methods allow us to understand the results concerning the stability of a nanomagnet without the need to introduce the bosonization of the quantum mechanical operators. The procedure performed here is richer since it allows us to obtain the quadratic Hamiltonian $\hat{H}_q$ describing the quantum fluctuations around equilibrium as well as the quantum properties of the states in equilibrium.

Let us now analyze the linear stability of the system in the nonrotating case (see Ref. [20] for the $\omega_S \neq 0$ case). The stability phase diagram derived using Eqs. (12) and (13) is shown in Fig. 2. This is a two-dimensional phase diagram with the x axis given by the bias field B_0 and the y axis given by the radius of the nanomagnet R. The remaining physical parameters are fixed; see the caption of Fig. 2. Two stable phases are found. The Einstein–de Haas (EdH) phase appears at low magnetic fields and for small radii. In this regime, the dynamics of the magnetization is dominated by the anisotropy interaction
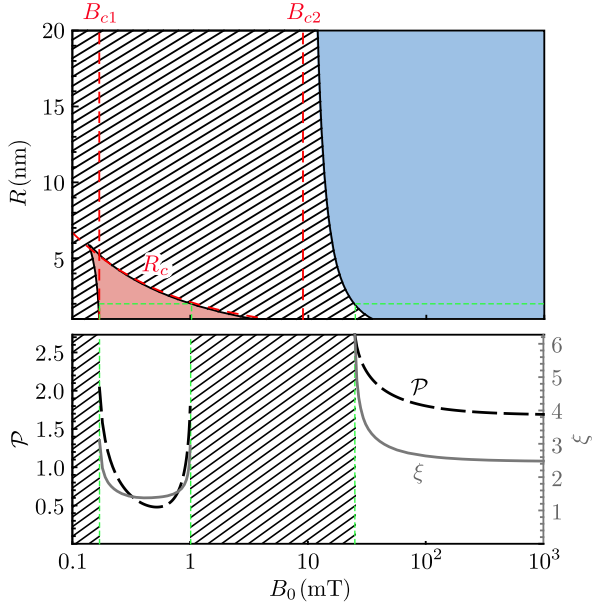
FIG. 2. (Top panel) Stability diagram for a nonrotating nanomagnet for $\rho_M = 10^4$ kg/m^3, $\rho_\mu = [\rho_M \mu_B/(50 \text{ amu})]$ J/(T m^3) (μ_B is the Bohr magneton and amu the atomic mass unit), $k_a = 10^4$ J/m^3, $B' = 10^4$ T/m, and $B'' = 10^6$ T/m^2. The red dashed lines represent the approximate borders $B_{c1} = 3[\hbar\rho_\mu B'^2/(4\mu_B\gamma_0\rho_M)]^{1/3}$, $R_c = \sqrt{5\rho_\mu/(8\gamma_0^2 B_0\rho_M)}$, and $B_{c2} = 2k_a\mu_B/(\hbar\gamma_0\rho_\mu)$ of the stable EdH phase (the red region) and the A phase (the blue region). (Bottom panel) Entanglement $\mathcal{P}$ (the black dashed line), and squeezing ξ (the gray solid line) of the quantum state $|0\rangle$ at the equilibrium as a function of B_0 in the stable regions for $R = 2$ nm (the green dashed lines in the stability diagram).

($\omega_D \gg \omega_L$). Because of the small moment-of-inertia-to-magnetic-moment ratio ($\omega_I \gg \omega_L$), the angular momentum contribution of the macrospin stabilizes the system through the Einstein–de Haas effect [1]. That is, the macrospin is locked along the anisotropy direction due to the conservation of energy [4,25,26]. Even if rotation is absent, the spin-rotation interplay described by the Einstein–de Haas effect stabilizes the nonrotating magnet by keeping the macrospin aligned along the anisotropy direction. The atom (A) phase appears at high magnetic field bias ($\omega_L \gg \omega_D$). In this regime, the nanomagnet behaves like a magnetic atom of mass M and spin S [11,12]: the anisotropy interaction can be neglected and the magnetic moment undergoes a free Larmor precession about the local magnetic field direction. The approximated expressions for the borders of the stable phases, given in the caption of Fig. 2, can be analytically obtained from the discriminant of the characteristic polynomials [20].

The stability diagram shows that a nonrotating nanomagnet can be stably levitated in a static field configuration. This opens up the possibility of cooling the thermal fluctuations of the degrees of freedom to the quantum

regime. The feasibility and analysis of such an experimental proposal will be addressed elsewhere. Let us now analyze the properties of the quantum state at the equilibrium in the absence of thermal fluctuations. This state corresponds to the vacuum state $|0\rangle$ of the normal eigenmodes of the quadratic Hamiltonian equation (10): $\hat{b}_Z$ and $\hat{c}_i$ for $i = 1, \ldots, 5$ ($[\hat{c}_i, \hat{c}_j^\dagger] = \delta_{ij}$). The c-bosonic modes $\hat{\boldsymbol{\Phi}} \equiv (\hat{c}_1, \hat{c}_1^\dagger, \ldots, \hat{c}_5, \hat{c}_5^\dagger)^T$ are obtained from modes $\hat{\boldsymbol{\Psi}}$ through a Bogoliubov transformation $\hat{\boldsymbol{\Phi}} = T^{-1}\hat{\boldsymbol{\Psi}}$ such that $T^\dagger M_T T = \text{diag}(\omega_1, \omega_1, \ldots, \omega_5, \omega_5)$ and $T^\dagger G T = G$. At each stable point of the phase diagram, the transformation T exists [27] and can be constructed as follows. One first obtains the eigenvalues λ_i and eigenvectors $\mathbf{v}_i$ (for $i = 1, \ldots, 10$) of K_T. At a stable point, K_T is diagonalizable and the λ_i values are real and nondegenerate. One then G orthonormalizes the eigenvectors such that, with an appropriate relabeling, they fulfill $\mathbf{v}_i^\dagger G \mathbf{v}_j = +\delta_{ij}$ for $i, j = 1, \ldots, 5$ and $\mathbf{v}_i^\dagger G \mathbf{v}_j = -\delta_{ij}$ for $i, j = 6, \ldots, 10$ [28]. The Bogoliubov transformation matrix is then given by $T = (\mathbf{v}_1 \mathbf{u}_1 \ldots \mathbf{v}_5 \mathbf{u}_5)$ (the vectors $\mathbf{v}_i$ and $\mathbf{u}_i$ are the columns of the matrix), where $\mathbf{u}_i \equiv (\sigma_x \otimes \mathbb{1}_5)\mathbf{v}_i^*$, with σ_x being the nondiagonal-real-valued Pauli matrix.

One can now analyze the properties of the vacuum state $|0\rangle$, which is a multimode Gaussian state, by the 10×10 covariance matrix [29]

$$\Theta_{ij} \equiv \frac{1}{2}\langle 0|(\hat{\Psi}_i\hat{\Psi}_j^\dagger + \hat{\Psi}_j^\dagger\hat{\Psi}_i)|0\rangle = \frac{1}{2}\sum_{k=1}^{10} T_{ik}(T^\dagger)_{kj}. \quad (15)$$

Note that the $\hat{b}_Z$-bosonic mode is not included in Θ since it is decoupled from all of the other modes. The five 2×2 diagonal blocks $(\Sigma_a)_{ij} \equiv \langle 0|(\hat{\varphi}_i\hat{\varphi}_j^\dagger + \hat{\varphi}_j^\dagger\hat{\varphi}_i)|0\rangle/2$ of Θ, with $\hat{\boldsymbol{\varphi}} \equiv (\hat{a}, \hat{a}^\dagger)$ and $\hat{a} = \hat{b}_L, \hat{b}_R, \hat{m}, \hat{k}, \hat{s}$, correspond to the covariance matrices of the a modes. The off-diagonal blocks describe the correlations between the modes. Entanglement in the pure state $|0\rangle$ can be quantified by $\mathcal{P} \equiv 5 - \sum_a \mathcal{P}_a$, where $\mathcal{P}_a = [2\sqrt{\det(\Sigma_a)}]^{-1}$ [30] is the purity of the a-bosonic mode. This characterizes the bipartite entanglement between one mode and the remaining four. Single-mode squeezing can be quantified via the squeezing parameter $\xi \equiv 1/\sqrt{2\min_k(\theta_k)}$, where θ_k represents the eigenvalues of Θ [29]. Figure 2 shows $\mathcal{P}$ and ξ as a function of B_0 for a given R in the stable phases. Bipartite entanglement and single-mode squeezing are thus present in the $|0\rangle$ state of a magnetically levitated nonrotating nanomagnet.

In conclusion, we showed that the quantum spin origin of the magnetization stabilizes magnetic levitation of a nonrotating nanomagnet, despite the Earnshaw theorem. Such a quantum spin stabilized levitation opens the door to experiments aiming not only at demonstrating the predicted phase diagram but also at bringing a nonrotating nanomagnet to the quantum regime, whose equilibrium states

show nontrivial quantum correlations. There are many directions left for further research, some of which we are currently addressing: the experimental proposal and feasibility analysis to prepare the $|0\rangle$ state by sympathetically cooling the degrees of freedom of a levitated nanomagnet near a flux dependent microwave cavity; the analysis and the potential applications (e.g., spin squeezing for magnetic sensing) of the quantum dynamics generated by placing the nanomagnet at the unstable regions of the phase diagram; levitating, coupling, and cooling several nanomagnets in the quantum regime to study quantum nanomagnetism in a unique substrate-free environment. We hope that such results and their potential applications will trigger further theoretical and experimental research to levitate nanomagnets in the quantum regime.

approximation, and (viii) dissipation-free dynamics for the system. Assumptions (iv)–(vi) could be easily relaxed with the same formalism. Assumptions (ii), (iii), and (vii) could be relaxed by considering internal phonons and other magnonic modes. Relaxing assumptions (i) and (viii) would most likely require a different analytical treatment.

[1] A. Einstein and W. J. De Haas, Proc. K. Ned. Akad. Wet. **181**, 696 (1915).

[2] S. J. Barnett, Phys. Rev. **6**, 239 (1915).

[3] M. Ganzhorn, S. Klyatskaya, M. Ruben, and W. Wernsdorfer, Nat. Commun. **7**, 11443 (2016).

[4] E. M. Chudnovsky, Phys. Rev. Lett. **72**, 3433 (1994).

[5] R. Jaafar, E. M. Chudnovsky, and D. A. Garanin, Phys. Rev. B **79**, 104410 (2009).

[6] R. Bassani, Meccanica **41**, 375 (2006).

[7] M. D. Simon, L. O. Heflinger, and S. L. Ridgway, Am. J. Phys. **65**, 286 (1997).

[8] H. R. Dullin and R. W. Easton, Physica (Amsterdam) **126D**, 1 (1999).

[9] S. Gov, S. Shtrikman, and H. Thomas, Physica (Amsterdam) **126D**, 214 (1999).

[10] M. V. Berry, Proc. R. Soc. A **452**, 1207 (1996).

[11] C. V. Sukumar and D. M. Brink, Phys. Rev. A **56**, 2451 (1997).

[12] D. M. Brink and C. V. Sukumar, Phys. Rev. A **74**, 035401 (2006).

[13] The model presented here is based on the following assumptions: (i) single magnetic domain, (ii) macrospin approximation, (iii) rigid body, (iv) sphere, (v) uniaxial anisotropy, (vi) Ioffe-Pritchard magnetic field, (vii) point-dipole

[14] S. Chikazumi and C. D. Graham, *Physics of Ferromagnetism* (Oxford University Press, Oxford, 2009).

[15] C. C. Rusconi and O. Romero-Isart, Phys. Rev. B **93**, 054427 (2016).

[16] For convenience, the total spin $\hat{\mathbf{S}}$ is defined as the negative of a standard spin operator such that its components satisfy anomalous commutation relations: the body (laboratory) frame components of $\hat{\mathbf{S}}$ satisfy $[\hat{S}_i, \hat{S}_j] = -i\epsilon_{ijk}\hat{S}_k$ ($[\hat{S}_\mu, \hat{S}_\nu] = -i\epsilon_{\mu\nu\lambda}\hat{S}_\lambda$) for i, j, $k = 1, 2, 3$ ($\nu, \mu, \lambda = x, y, z$) [15].

[17] We assume that the magnetization arises from the electron spins, for which $\gamma_0 = 1.760$ rad T^{-1} s^{-1}.

[18] D. Gatteschi, R. Sessoli, and J. Villain, *Molecular Nanomagnets* (Oxford University Press, New York, 2011).

[19] J. Reichel and V. Vuletic, *Atom Chips* (Wiley-VCH Verlag, Weinheim, 2011).

[20] C. C. Rusconi, V. Pöchhacker, J. I. Cirac, and O. Romero-Isart, Phys. Rev. B **96**, 134419 (2017).

[21] J. D. Meiss, *Differential Dynamical Systems* (Society for Industrial and Applied Mathematics, Philadelphia, 2008).

[22] A. Klein and E. R. Marshalek, Rev. Mod. Phys. **63**, 375 (1991).

[23] The fact that $\hat{J}_3$ and $\hat{J}_z$ commute corresponds to the classical result that a rotating top has, at most, two conserved directions of the angular momentum: the precession about $\mathbf{e}_z$ and the mechanical rotation about $\mathbf{e}_3$. See Ref. [15] for a proof showing that $[\hat{J}_3, \hat{J}_z] = 0$.

[24] T. Holstein and H. Primakoff, Phys. Rev. **58**, 1098 (1940).

[25] E. M. Chudnovsky and D. A. Garanin, Phys. Rev. B **81**, 214423 (2010).

[26] M. F. O'Keeffe and E. M. Chudnovsky, Phys. Rev. B **83**, 092402 (2011).

[27] O. Maldonado, J. Math. Phys. (N.Y.) **34**, 5016 (1993).

[28] Since the eigenvalues are all distinct, the eigenvectors $\mathbf{v}_i$ are already G orthogonal, and they need only to be properly normalized.

[29] R. Simon, N. Mukunda, and B. Dutta, Phys. Rev. A **49**, 1567 (1994).

[30] M. G. A. Paris, F. Illuminati, A. Serafini, and S. De Siena, Phys. Rev. A **68**, 012314 (2003).